A Passive Variable Impedance Control Strategy with Viscoelastic Parameters Estimation of Soft Tissues for Safe Ultrasonography

Luca Beber[1], Edoardo Lamon[2,3], Davide Nardi[2], Daniele Fontanelli[1], Matteo Saveriano[1], Luigi Palopoli[2]

***Abstract*— In ultrasonography, robots have the potential to reproduce the skills required to acquire high-quality images while reducing the sonographer's physical efforts. In this paper, we present a variable impedance strategy to control the interaction of the probe with the patient's body while ensuring safety and passivity even in cases of sudden contact loss.**

I. Introduction

Acquiring ultrasound images is a complex task that requires skilled sonographers and the continuous exertion of considerable force, which might result in a health risk. The quality of the diagnosis very much depends on the skills of the sonographer, and the number of experienced operators is not sufficient to deliver the service in remote areas [1]. Robotised solutions have the potential to eliminate such issues. A crucial aspect is how to control the motion of the probe along trajectories on the patient's body. The literature in this area offers both autonomous [1] and teleoperated [2] solutions. While the two approaches differ mainly on position reference computation, both require the regulation of the contact forces with the patient's body. An example of this is when the patient moves or there is a contact loss between the probe tip and the patient's body, which might be caused by the presence of a gel that removes the friction of the surface.

In this paper, we focus on the problem of force-controlled motion for lung and heart ultrasonography. At the core of our approach is a method to optimise on-the-fly the impedance parameters of a compliant controller [3] by exploiting the paradigm of variable impedance control. The optimisation problem is formulated through quadratic programming (QP) and includes physical constraints, which are obtained by means of a prior estimation of the viscoelastic parameters, and safety constraints through the addition of an energy tank. To initialise the proposed control strategy, an offline phase is required, which consists of a discrete biomechanics characterisation and a smoothing operation to retrieve a continuous body description.

II. Methodology

A. Tissue Parameters Estimation

Biological tissues are known to demonstrate viscoelastic behaviour, implying that their response depends not only on the deformation applied but also on the rate of deformation. As a result, they can be represented using springs and dampers arranged in various configurations. The most used model is the Kelvin-Voight (KV), where the tissue is modelled with a spring damper-system. Similarly, an energetically correct model is Hunt-Crossley (HC) [4], [5]:

$$F_{tissue}(t) = \begin{cases} \kappa\varepsilon^{\beta}(t) + \lambda\varepsilon^{\beta}(t)\dot{\varepsilon}(t), & \varepsilon \geq 0 \\ 0, & \varepsilon < 0 \end{cases}, \tag{1}$$

where $\varepsilon(t) \in \mathbb{R}$ is the amount of penetration, $\dot{\varepsilon}(t) \in \mathbb{R}$ is the penetration rate, $\kappa \in \mathbb{R}$ is the elasticity, and $\eta \in \mathbb{R}$ is the viscosity. $\beta \in (1.0, 1.5)$ are generally reasonable values for biological tissue. The stiffness and damping parameters for a point on a surface can be estimated using the least square method by palpating the body with a sinusoidal motion. A 3D map of the inspected surface can be created by repeating the dynamic test at different points on the body. An elasticity and viscosity map of the area can then be built using a Gaussian process regression (GPR).

B. Variable Impedance Control

The stability of a variable impedance system might be violated in the presence of a variable impedance controller. The passivity of the system can be enforced through the concept of passivity of the power port $\dot{\boldsymbol{x}}^T\boldsymbol{F}^{ext}$. To do so, we introduce the formalism of port-Hamiltonian systems to describe the interaction model of the variable Cartesian impedance augmented with an energy tank with dynamics:

$$\dot{\mathrm{x}}_t = \frac{\sigma}{\mathrm{x}_t}\dot{\tilde{\boldsymbol{x}}}^T\boldsymbol{D}^d\dot{\tilde{\boldsymbol{x}}} - \frac{\boldsymbol{w}^T}{\mathrm{x}_t}\dot{\tilde{\boldsymbol{x}}}, \tag{2}$$

where $\mathrm{x}_t \in \mathbb{R}$ is the state of the tank, $\sigma \in \{0, 1\}$ modulates the energy storage, and $\boldsymbol{w}$ an the extra input of the port-Hamiltonian system defined as:

$$\boldsymbol{w}(t) = \begin{cases} -\boldsymbol{K}^v(t)\tilde{\boldsymbol{x}} & \text{if } T(\mathrm{x}_t) > T_{min} \\ 0 & \text{otherwise,} \end{cases} \tag{3}$$

where $\boldsymbol{K}^v(t)$ is time-varying component of the stiffness ($\boldsymbol{K}^d(t) = \boldsymbol{K}^{min} + \boldsymbol{K}^v(t)$). At each instant of time, the tank energy is defined by $T(\mathrm{x}_t) = \frac{1}{2}\mathrm{x}_t^2$ and $T_{min} \in \mathbb{R}^+$ is the minimum energy that the tank is allowed to store. Thanks to (3), we can infer the condition $T(\mathrm{x}_t) > T_{min}$ when the stiffness is allowed to raise without violating the passivity constraint. However, this bound does not prevent the energy of the tank to be drained instantaneously, situation which leads to the complete loss of performance. For this reason, it is reasonable to further constrain the power flow of the tank when the energy is extracted from the tank ($\dot{T}(\mathrm{x}_t) > \eta$), where $\eta \in \mathbb{R}^-$ is the maximum allowed power.

[1]Department of Industrial Engineering, Università di Trento, Trento, Italy.
[2]Department of Information Engineering and Computer Science, Università di Trento, Trento, Italy. luca.beber@unitn.it
[3]Human-Robot Interfaces and Interaction, Istituto Italiano di Tecnologia, Genoa, Italy.

A QP optimisation problem can be constructed to involve a trade-off between the precise tracking of a desired wrench and the necessity to uphold a limited level of stiffness [6]. The QP is formulated as follows:

$$
\begin{aligned}
&\min_{\boldsymbol{K}^d \in \mathbb{R}^{m\times m}} \frac{1}{2}\left(\|\boldsymbol{F}^{ext} - \boldsymbol{F}^d\|^2_{\boldsymbol{Q}} + \|\boldsymbol{K}^d - \boldsymbol{K}^{min}\|^2_{\boldsymbol{R}}\right)\\
&\text{s.t. } \boldsymbol{K}^{min} \preccurlyeq \boldsymbol{K}^d \preccurlyeq \boldsymbol{K}^{max}\\
&\quad\;\; \boldsymbol{F}^{min} \preccurlyeq \boldsymbol{F}^{ext} \preccurlyeq \boldsymbol{F}^{max}\\
&-\tilde{\boldsymbol{x}}^T \boldsymbol{K}^d \dot{\tilde{\boldsymbol{x}}} \le \sigma \dot{\tilde{\boldsymbol{x}}}^T \boldsymbol{D}^d \dot{\tilde{\boldsymbol{x}}} - \tilde{\boldsymbol{x}}^T \boldsymbol{K}_{min} \dot{\tilde{\boldsymbol{x}}} + \frac{T_{t-1} - T_{min}}{\Delta t}\\
&-\tilde{\boldsymbol{x}}^T \boldsymbol{K}^d \dot{\tilde{\boldsymbol{x}}} \le \sigma \dot{\tilde{\boldsymbol{x}}}^T \boldsymbol{D}^d \dot{\tilde{\boldsymbol{x}}} - \tilde{\boldsymbol{x}}^T \boldsymbol{K}_{min} \dot{\tilde{\boldsymbol{x}}} - \eta
\end{aligned}
\tag{4}
$$

where $\boldsymbol{Q}$ and $\boldsymbol{R} \in \mathbb{R}^{m\times m}$ are diagonal positive definite weighting matrices, $\boldsymbol{K}^d \in \mathbb{R}^{m\times m}$ is the desired stiffness of the Cartesian impedance controller, $\boldsymbol{K}^{min}$ and $\boldsymbol{K}^{max} \in \mathbb{R}^{m\times m}$ are diagonal matrices representing the minimum and maximum allowed stiffness, $\boldsymbol{F}^{ext} \in \mathbb{R}^m$ is the wrench of the impedance interaction model, $\boldsymbol{F}^d \in \mathbb{R}^m$ is the desired interaction wrench and $\boldsymbol{F}^{max}/\boldsymbol{F}^{min} \in \mathbb{R}^m$ is the maximum/minimum wrench that the robot can exert. The symbol $\preccurlyeq$ represents the matrix inequality. The last two constraints limit the maximum energy $T - T_{min}$ which can be injected in the system and the rate $|\eta|$ at which the energy is injected, and are obtained from $T \ge T_{min}$ and $\dot{T} \ge \eta$. $1/\Delta t$ is the controller frequency. Given the formulation of the optimisation problem in (4), in this paper we propose two strategies to set the desired and the minimum force, $\boldsymbol{F}^d$ and $\boldsymbol{F}^{min}$ in the problem according to (1). From now on, we will focus on the vertical component of these forces, denoted as $F_{z,d}$ and $F_{z,min}$. The two strategies are defined as follows:

1) Variable Stiffness with Constant Force (*VS-CF*): $F_{z,d} = F^{ref}_{body}$ constant and $F_{z,min}(\varepsilon_{max})$,
2) Variable Stiffness with Variable Force (*VS-VF*): $F_{z,d} = F_{body}(\varepsilon_d)$ and $F_{z,min}$ constant.

In VS-CF the objective is to achieve a reference force, similar to what happens in force control. This force is constrained, however, to meet the condition of maximum penetration that the end effector can have in the body. This constraint is expressed in the minimum force that can be generated, i.e.,

$$F_{z,min}(\varepsilon_{max}, x, y) = \kappa_{x,y}\varepsilon^{\beta}_{max} + \lambda_{x,y}\dot{\varepsilon}\varepsilon^{\beta}_{max}, \tag{5}$$

where $\kappa_{x,y}$ and $\lambda_{x,y}$ are the values of the HC model at that point, and ε_{max} is the maximum penetration. We assume that the stiffness of the body is constant up to a certain depth, so it is not necessary to reach ε_{max} at each palpation during the estimation phase, which may not be clinically safe. The penetration velocity $\dot{\varepsilon}$ can be rewritten in function of end effector velocity and surface change in the direction of movement $\boldsymbol{d}$ as

$$\dot{\varepsilon} = -\dot{z}_{ee} - \nabla z(x, y) \cdot \boldsymbol{d}. \tag{6}$$

This formulation prevents the robot from sinking excessively into the softest parts of the body, adding another degree of safety in addition to those provided by the energy tanks and energy valves. *VS-VF* can be seen as the opposite approach to *VS-CF*, as it tries to maintain the desired penetration along the entire trajectory but avoid crossing the ribs because the force exerted is excessive and thus may injure the patient. The equation that describes the desired force is similar to (5), but instead of using a ε_{max} that has to be avoided, ε_d will be used, that should be kept over all the trajectory.

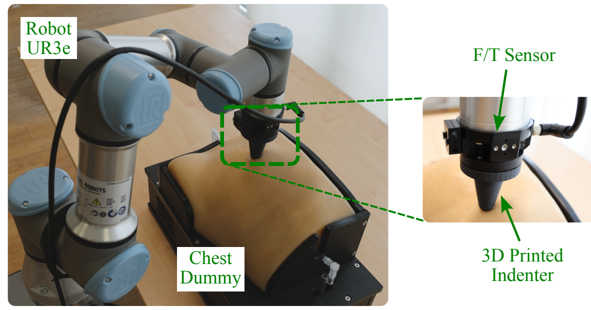

Fig. 1. Experimental setup.

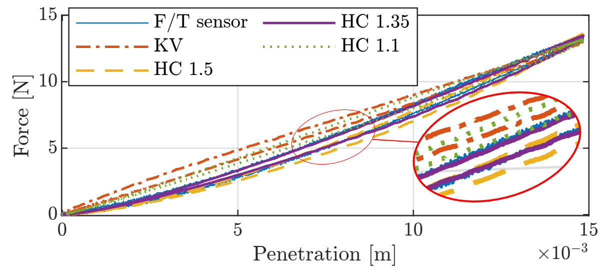

Fig. 2. Load tests obtained with the different models.

III. Experimental Results

A. Viscoelastic Model Validation

A load test was performed to validate the soft body model Figure 1. The HC model with β=1.35 obtained lower relative residuals error with respect to the measured force (Figure 2). The palpations on the chest dummy were made at a distance of 1 cm apart so that the surface could be accurately reconstructed. The GPR is used to build an elasticity and viscosity map based on the position in the 3D space. Focusing on the elasticity map, in Figure 4, it can be seen that the method is able to detect the presence of stiffer areas, which represent the ribs of the chest dummy. In Figure 5 the dummy-specific elasticity map is projected on the surface reconstructed with the `GRIDFIT` algorithm [7]. The upward tilt in the bottom left of the figure is the beginning of the shoulder. It is interesting to notice that the rib covered by the pectoral muscle seems less stiff than the others covered only by a thin layer of skin.

B. Variable Impedance Control Validation

In the validation of our control (*VS*) we compare its performances against other control strategies such as a force control (*CF*) and a classical impedance control (*CS*). For the controller validation experiments, a reference target is maintained at constant z under the surface of the dummy. Note that the *CF* is hybrid since the x and y axes are controlled by the compliant controller, while the z axis is

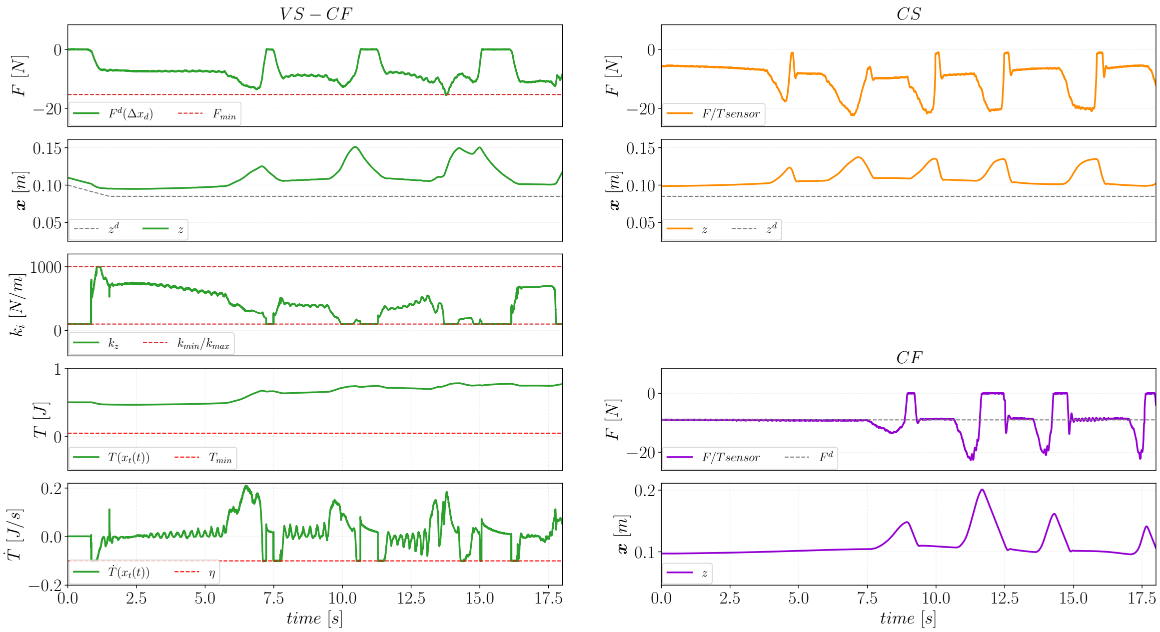

Fig. 3. Ultrasound experiment on a dummy chest with disturbances.

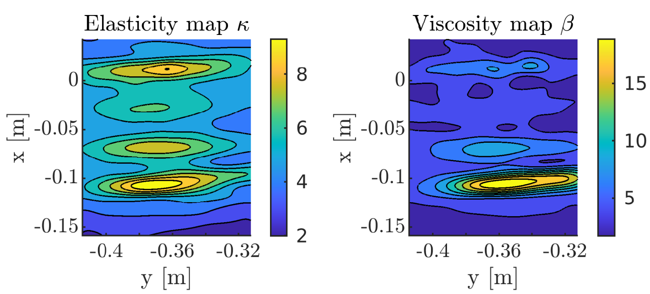

Fig. 4. Elasticity and viscosity maps obtained with GPR.

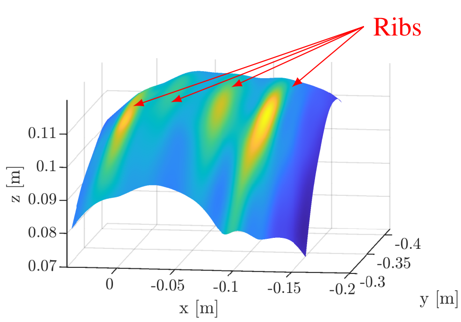

Fig. 5. Surface reconstruction with elasticity information.

controlled in force. As expected, the force generated by the *CS* control is strongly dependent on the shape of the body: when the surface is further from the target, the generated force is stronger than when the surface is closer. The force controller, instead, can track the target force without any problem but has the downside that it cannot be controlled in position. The controller can track a reference force as good as a force control keeping the ability to control the axis in which the force is generated. On top, it uses the information registered by the reconstruction to cut the reference force when the maximum penetration is reached preventing the tip from sinking further. The same test is done under the action of some disturbances to demonstrate the inherent safety of this new approach Figure 3. The disturbance consists of raising the dummy to see how the control would handle the situation. As soon as the end-effector starts to be moved away, the stiffness of the impedance spring starts decreasing until no force is acting anymore; then, the spring value is limited to its minimum until the moment of the new contact. At the moment of contact, the stiffness would suddenly increase, but the presence of the valves partially limits its growth and restricts the tank from being emptied too quickly.

IV. Conclusion

This paper presents a novel variable impedance strategy to regulate the interaction forces between the probe and the patient's body in ultrasonography operations. This is particularly useful in the case of lung or heart ultrasounds where ribs and muscles are close. Furthermore, to ensure the stability of the variable impedance, the energy tank was used to ensure the passivity of the system and prevent unsafe behaviour by limiting the minimum energy and the maximum power flow. The experimental results show that the proposed controller outperforms the baseline regarding tracking performance and safety.

References

[1] K. Li *et al.*, "An Overview of Systems and Techniques for Autonomous Robotic Ultrasound Acquisitions," *IEEE Transactions on Medical Robotics and Bionics*, vol. 3, no. 2, pp. 510–524, 5 2021.

[2] F. von Haxthausen *et al.*, "Medical Robotics for Ultrasound Imaging: Current Systems and Future Trends," *Current Robotics Reports*, 2021.

[3] S. Scherzinger *et al.*, "Forward Dynamics Compliance Control (FDCC): A new approach to cartesian compliance for robotic manipulators," in *IEEE IROS*, vol. 2017, 12 2017, pp. 4568–4575.

[4] N. Diolaiti, C. Melchiorri, and S. Stramigioli, "Contact impedance estimation for robotic systems," *IEEE Transactions on Robotics*, vol. 21, no. 5, pp. 925–935, 10 2005.

[5] K. H. Hunt and F. R. Crossley, "Coefficient of Restitution Interpreted as Damping in Vibroimpact," *Journal of Applied Mechanics*, vol. 42, no. 2, pp. 440–445, 6 1975.

[6] S. Hjorth, E. Lamon, D. Chrysostomou, and A. Ajoudani, "Design of an Energy-Aware Cartesian Impedance Controller for Collaborative Disassembly," *Proceedings - IEEE International Conference on Robotics and Automation*, 2 2023.

[7] J. D'Errico, "Surface fitting using gridfit," *MATLAB central file exchange*, vol. 643, 2005.